

SYNTHESIS OF A NEW COBALT PYROCATECHIN DIANION COMPLEX AND INVESTIGATION OF THE KINETICS OF ITS REDOX-ACTIVATED DISSOCIATION

© 2025 E. A. Khakina^{a,*}, I. A. Nikovsky^a, A. A. Danshina^{a, b},
E. P. Antoshkina^{a, b}, A. N. Rodionov^a, and Yu. V. Nelyubina^a

^a*A. N. Nesmeyanov Institute of Organoelement Compounds, Russian Academy of Sciences, Moscow, Russia*

^b*Moscow Institute of Physics and Technology (National Research University), Dolgoprudny, Moscow Region, Russia*

*e-mail: khakina90@ineos.ac.ru

Received April 27, 2024

Revised April 16, 2024

Accepted April 16, 2024

Abstract. A new redox-active cobalt(III) complex with pyrocatechin dianion and two 4,4'-dimethoxy-2,2'-bipyridine molecules as ligands was synthesized. The *in situ* reduction of the synthesized complex by ascorbic acid in an inert atmosphere was studied using *in situ* NMR spectroscopy. It is shown that this process is of the first order in the initial complex with a rate constant of $1.1 \times 10^{-3} \text{ s}^{-1}$ and is accompanied by the release of em pyrocatechin, which acts as a model drug.

Keywords: *in situ nuclear magnetic resonance spectroscopy, pyrocatechin, cobalt complexes, redox-activated drug delivery*

DOI: 10.31857/S0132344X250107e8

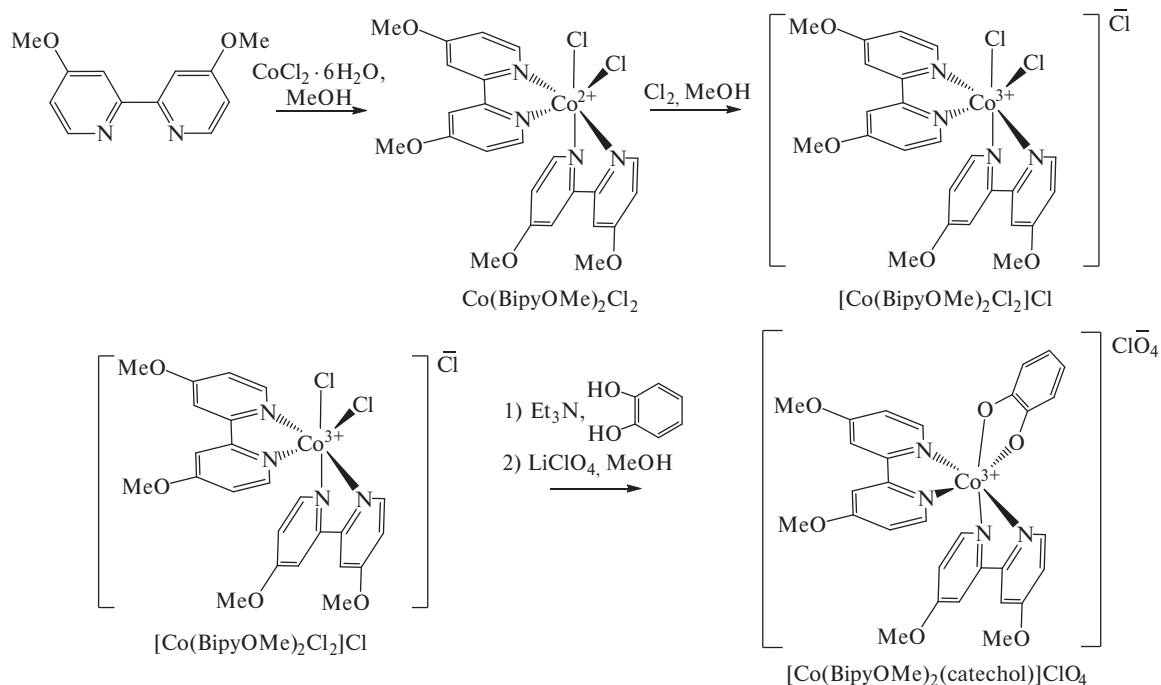
INTRODUCTION

Cancer is one of the top ten leading causes of death in people under the age of 70, according to the World Health Organization, prompting scientists to look for new treatments. в опухолевых тканях Biogenic reducing agents, such as ascorbic acid, glutathione, and cysteine, accumulate in cells and create an environment with a low oxygen content (hypoxic regions) due to impaired metabolism in tumor tissues [1]. Hypoxia significantly reduces the effectiveness of radiotherapy for solid tumors [2]. However, differentiation of cancer-affected and healthy tissues by oxygen level became the basis for developing a strategy of redox-activated drugs that act selectively on tumor cells [3]. The use of hypoxia-activated prodrugs can not only increase the effectiveness of cancer treatment, but also reduce the negative side effects of chemotherapy, providing cytotoxicity only in tumor cells [4].

Metal complexes are actively studied as “molecular platforms” for targeted delivery of anti-cancer drug molecules to tumor cells [5]. Cobalt complexes are of particular interest from this point of view. Cobalt(III) complexes are characterized by a sufficiently large stability constant, which ensures their inertia when ingested [6]. The correct selection of ligands makes it possible to obtain complexes with

the redox potential of Co(III)/Co(II) in the range of potentials of biological intracellular reductants [7]. Cobalt(II) complexes formed during reduction are capable of eliminating one of the ligands [6]. This stage just leads to the release of the drug molecule. In addition, the reduction of the cobalt ion leads to a sharp change in its magnetic properties: the Co(III)/Co(II) transition is accompanied by the formation of a paramagnetic cobalt ion, which makes it possible to track the release of the drug using MRI [8].

Many heteroleptic cobalt(III) complexes with anti-cancer drug molecules as ligands, x such as *bis*(2-chloroethyl)amine [9], N, N' -*bis*(chloroethyl)ethylenediamine [10], marimastate [11], 8-hydroxyquinoline [12], azachloromethylbenzindoline [13], and erlotinib [14] were investigated as hypoxia-activated prodrugs. Despite some promising results in *in vitro* experiments, attempts to reproduce them *in vivo* have not been successful due to the complex metabolism of these complexes in living organisms and the difficulties of modeling drug release in a hypoxic living cell. Another reason may be a lack of understanding of how to control the kinetics of drug release to enhance anti-cancer activity by chemical modification of ligands, even *in vitro*, which precludes the molecular design of cobalt(III) complexes as hypoxia-activated



Scheme 1

prodrugs. This makes it necessary to conduct systematic studies to establish the regularities of the redox activation process for further optimization of prodrugs based on cobalt complexes.

One of the factors that significantly affects the therapeutic effect of drug delivery using “molecular platforms” is the rate of recovery of the cobalt ion in the complex and the subsequent release of the drug. If recovery is too slow, there is a risk that the complex will be eliminated from the body before a sufficient amount of the drug is released into the tumor cells. It is known that the structure of ligand affects the energy of the molecular orbitals of complexes and, as a consequence, their redox potential [15], which makes it possible to optimize the process of drug release during восстановлении комплекса reduction of cobalt complexes by changing the structure of the ligands that make up their composition.

Previously, we proposed an approach that allows monitoring the processes of redox activation of drugs in cobalt(III) complexes *in situ* using NMR spectroscopy. This allowed us to study the reduction by ascorbic acid of heteroleptic cobalt(III) complexes containing 2,2'-bipyridine or 1,10-phenanthroline and 2-oxo-2*H*-chromene-6,7-diolate dianion as ligands [16], and to find that the complex with phenanthroline is reduced much faster. Also, using the proposed approach, two cobalt complexes with different model drugs (6,7-dihydroxycoumarin and pyrocatechin) and bipyridine ligands were shown to have a significant effect on the reduction rate

due to the structure of the eliminated ligand [17]. When comparing the reduction rate of cobalt(III) complexes with bipyridine ligands and the 6,7-dihydroxycoumarin dianion, it was shown that the introduction of methoxy substituents into the aromatic core of bipyridine leads to a decrease in the reduction rate of the corresponding complex and, as a consequence, a decrease in the release rate of 6,7-dihydroxycoumarin [17, 18].

In this paper, we synthesized a new redox-active cobalt(III) complex $[\text{Co}(\text{BipyOMe})_2(\text{catechol})]\text{ClO}_4$ (**I**) containing 4,4'-dimethoxy-2,2'-bipyridine and pyrocatechin dianion (with schema 1) as ligands, and its reduction by ascorbic acid *in situ* was studied by NMR spectroscopy. Pyrocatechin, the dianion of which is part of **I**, acts as a model drug, since it is a structural fragment of many biologically active compounds – antioxidants, epinephrine, etc. The reduction rate of the synthesized complex **I** was compared with the reduction rate of the $[\text{Co}(\text{Bipy})_2(\text{catechol})]\text{ClO}_4$ complex, which was studied earlier [17], to determine the effect of the introduction of methoxy groups into the aromatic core of bipyridine on the reduction rate of the corresponding complex and the rate of pyrocatechin release.

THE EXPERIMENTAL PART

As a precursor for the synthesis of the cobalt complex $[\text{Co}(\text{BipyOMe})_2(\text{catechol})]\text{ClO}_4$ (**I**) was used

for the cobalt(III) complex $[\text{Co}(\text{BipyOMe})_2\text{Cl}_2]\text{Cl}$ (II) obtained by oxidation of the corresponding cobalt(II) complex with chlorine gas [19]. Chlorine was obtained by reacting potassium permanganate with concentrated hydrochloric acid and was dried by passing it through concentrated sulfuric acid [20]. Commercially available 4,4' – dimethyl-2,2' – bipyridine (97%, Sigma-Aldrich), cobalt (II) chloride hexahydrate (98%, Sigma-Aldrich), pyrocatechin (98%, Sigma-Aldrich), lithium perchlorate (98%, Alfa Aesar), triethylamine (99%, Sigma-Aldrich) was used without pretreatment.

Synthesis of the complex $[\text{Co}(\text{BipyOMe})_2\text{Cl}_2]\text{Cl}$ (II). A solution of 4,4'-dimethyl-2,2'-bipyridine (1,681 mmol; 363 mg) in methanol was added to a solution of cobalt(II) chloride hexahydrate (0.84 mmol; 200 mg) in 10 ml of methanol. The resulting mixture was boiled for 2 h. During this time, the color of the solution changed from yellow to red-brown. The reaction mixture was then cooled to room temperature and bubbled through it with chlorine gas obtained by reacting potassium permanganate with concentrated hydrochloric acid. In this case, the target complex was formed in the form of a crystalline green precipitate. The precipitate was separated by filtration, washed with ethanol, and dried in vacuum. The yield is 362 mg (72%).

NMR ^1H (CD_3OD , 300 MHz; δ , ppm): 9.63 (d, $J = 6.9$ Hz, 2H, Sn), 8.34 (d, $J = 2.6$ Hz, 2H, Sn), 8.16 (d, $J = 2.6$ Hz, 2H, SH), 7.64 (dd, $J = 6.9, 2.6$ Hz, 2H, SH), 7.21–6.92 (m, 4H, SH), 4.21 (s, 6H, OSH_3), 3.98 (s, 6H, OSH_3).

Mass spectrum (ESI), m/z : $[\text{Co}(\text{BipyOMe})_2\text{Cl}_2]^+$, calculated 561.1, found 560.9.

Synthesis of the complex $[\text{Co}(\text{BipyOMe})_2(\text{catechol})\text{ClO}_4]$ (I). A solution of pyrocatechin (0.5 mmol; 55 mg) and triethylamine (1 mmol; 101.2 mg; 139 μl) in 10 ml of methanol was added to the solution of $[\text{Co}(\text{BipyOMe})_2\text{Cl}_2]\text{Cl}$ (0.5 mmol; 299 mg) in 15 ml of methanol. The resulting mixture was boiled for 3 hours, then cooled to room temperature, a solution of lithium perchlorate (1.25 mmol; 133 mg) was added in 5 ml of methanol and stirred for 30 minutes while cooling in a water bath to crystallize the target complex. The resulting green precipitate was separated by filtration, washed with isopropanol and diethyl ether, and dried at reduced pressure. The yield is 255 mg (73%).

NMR ^1H (CD_3) NMR: DMSO-d_6 10: 1 vol.; 400 MHz; δ , ppm): 8.59 (d, $J = 6.7$ Hz, 2H, SN), 8.2222 (d, $J = 2.7.7$ Hz, 2H, SN), 8.1515 (d, $J = 2.7.7$ Hz, 2H, Sn), 7.3737 (DD, $J = 6.7, 2.7$ Hz, 2H, Sn), 7.2222 (d, $DD, J = 6.4.4$ Hz, 2H, Sn), 6.96.96 (DD, $J = 6.6.6, 2.8.8$ Hz, 2H, Sn), 6.45–6.41 (m, 2H, SN), 6.24–6.19 (m, 22H, SN), 4.0707 (s, 6H, OSN_3), 3.98.98 (s, 6H, OSN_3). **ЯМР** ^{13}C (CD_3) NMR: DMSO-d_6 10: 1 rev; 101 MHz; δ , ppm: 170.7575, 170.1414, 160.91.91, 158.64.64, 158.41.41, 152.79.79, 151.51.51, 117.53.53, 115.76.76, 114.65.65, 114.46.46, 112.36.36, 111.63, 58.02.02, 57.9191.

Mass spectrum (ESI), m/z : found 599.1338, 383.0431; calculated for $\text{C}_{30}\text{H}_{28}\text{CoN}_4\text{O}_6$ $[\text{Co}(\text{BipyOMe})_2(\text{catechol})]^+$ 599.1335, for $\text{C}_{18}\text{H}_{16}\text{CoN}_2\text{O}_4$ $[\text{Co}(\text{BipyOMe}) (\text{catechol})]^+$ 383.0437.

Preparation of the complex $[\text{Co}(\text{BipyOMe})_3](\text{ClO}_4)_2$ (III). A solution of cobalt(II) perchlorate hexahydrate (4.1 mg; 0.011 mmol) in 0.55 ml of deuterated acetonitrile was added to dry 4,4'-dimethoxy-2,2'-bipyridine (7.3 mg; 0.034 mmol). The resulting mixture was stirred using a vortex until 4,4'-dimethoxy-2,2'-bipyridine was completely dissolved, 150 μl of deuterated water was added and were added to the NMR ampoule for recording the spectrum without isolation.

NMR ^1H (CD_3CN : D_2O 5: D_2O 5: 1 vol; 400 MHz; δ , ppm.); 93.93 (us.s, 6H, Sn), 78.6060 (us.s, 6H, Sn), 41.57.57 (us.s, 6H, SN), 6.64.64 (us.s, 18H, SN_3).

Mass spectrum (ESI), m/z : $[\text{Co}(\text{BipyOMe})_3]^{2+}$, calculated 353.6.6, found 353.6.6.

Spectra of NMR ^1H and ^{13}C of cobalt complexes were recorded for solutions in deuterated methanol and acetonitrile using Bruker Avance 300 and Varian Inova 400 NMR spectrometers with an operating frequency for protons of 300.15 and 400.1313 MHz, respectively. The values of chemical shifts were determined relative to the signals of residual solvent protons (^1H 3.31 ppm, ^{13}C 49.0 ppm for CD_3OD ; ^1H 1.94 ppm, ^{13}C 1.32 ppm for CD_3CN).

Mass spectrometric analysis of complexes II, III and reduction products of complex I was performed using a liquid chromatography-mass spectrometer model LCMS-2020 (Shimadzu, Japan) with electrospray ionization and a quadrupole detector (registration of positive and negative ions with m/z in the range of 50–2000–). The electrospray voltage was 4.5 kV, and the temperatures of the desolvation line and the heating unit were 250 and 400°C, respectively. Nitrogen (99.5%) was used as the spray and drying gas, and acetonitrile (99.9+%, Chem-Lab) was used as the mobile phase with a flow rate of 0.4 ml/min. The volume of the analyzed sample is 0.5 μl .

High-resolution mass spectra of complex I were recorded using an LCMS-9030 liquid chromatography-mass spectrometer (Shimadzu, Japan) with electrospray ionization and a tandem quadrupole-time-of-flight mass analyzer (recording positive ions with m/z in the range of 100–2000–). The electrospray voltage was 4.5 kV, and the interface, desolvation line, and heating unit temperatures were 300, 250, and 400°C, respectively. Nitrogen (99.5%) was used as the heating gas (10 l/min), spray gas (3 l/min), and drying gas (10 l/min), while the mobile phase was acetonitrile (99.9+%, Chem-Lab) with a flow rate of 0.4 ml/min. The volume of the analyzed sample is 0.05 μl . A solution of sodium iodide mixed with methanol and water was used as an external calibration standard.

PCA of single crystals of the complex I was conducted on a Bruker Quest D8 CMOS diffractometer (MoK α

Table 1. Basic crystallographic data and parameters of refinement of the structure of $[\text{Co}(\text{BipyOMe})_2(\text{catechol})]\text{ClO}_4$ (I)

Parameter	Value
Gross value formula	$\text{C}_{30}\text{H}_{33.20}\text{ClCoN}_4\text{O}_{12.60}$ $\text{C}_{30}\text{H}_{28}\text{N}_4\text{O}_6\text{Co}, 2(\text{C}_{10.5}\text{O}_2), 2.6(\text{H}_2\text{O}_2)$
Molecular weight	745.78
T, K	100
Crystal system	Monoclinic
Space group	$C2/c$
Z	4
$a, \text{\AA}$	12.3125 (3)
$b, \text{\AA}$	14.9493(3)
$c, \text{\AA}$	17.8258(4)
α, deg	90
β, deg	99.0600(10)
γ, deg	90
$V, \text{\AA}^3$	3240.14(13)
ρ (ext.), g cm^{-3}	1.529
μ, cm^{-1}	6.84
$F(000)$	1544
$2\theta_{\text{max}}, \text{deg}$	58
Number of measured reflections	21548
Number of independent reflections	4306
Number of reflections with $I > 3\sigma(I)$	3402
Number of specified parameters	226
R_1	0.0666
wR_2	0.1928
GOOF	1.040
Residual electron density ($d_{\text{max}}/d_{\text{min}}$), e \AA^{-3}	1.525/-1.6991.699

radiation, graphite monochromator, ω -scanning). The structure was decoded using the ShelXT program ShelXT[21] and refined in the full-matrix OLS using the Olex2 program [22] in the anisotropic approximation in F^2_{hkl} . The positions of hydrogen atoms are calculated geometrically, and they are refined in an isotropic approximation using the rider model. Too much disordered water molecules were considered as a diffuse contribution to the total scattering without taking into account specific atomic positions using the Solvent Mask procedure in Olex2 [22]. The main crystallographic data and refinement parameters are presented in Table. 1.

Structural data for the complex is deposited in the Cambridge Structural Data Bank (CCDC # 2350158; <http://www.ccdc.cam.ac.uk/>).

For *in situ* spectroscopy NMR complex I (10 mmol; 7.00 mg), ascorbic acid (20 mmol; 3.6 mg), 550 μl CD_3CN , and 3 μl dibromomethane (internal standard) were placed in an ampoule with a screw cap and septa. The ampoule was then frozen in liquid nitrogen, evacuated, and filled with argon.

For the initial mixture the NMR spectrum ^1H was registered at 40°C on a Bruker Avance 300 spectrometer with an operating frequency for protons of 300.15 MHz. The values of chemical shifts (δ, ppm) were determined relative to the residual solvent signal ($^1\text{N}1.94 \text{ ppm}$ for CD_3CN). The following recording parameters were used: the spectrum range was 150 ppm, the recording time was 0.2 s, the relaxation delay duration was 0.6 s, the pulse duration was 9.5 microseconds, and the number

of accumulations was 32. The resulting free induction drops were processed to increase the signal-to-noise ratio by exponential weighting with a coefficient of up to 1. Then, 150 μ l of D₂o was added through the septa using a syringe D₂, and the mixture was shaken until ascorbic acid was completely dissolved. Further registration of NMR spectra was performed every two minutes for 40 minutes at a temperature of 40°C using parameters similar to the registration of the spectrum of the initial mixture. The conversion rate was estimated by the consumption of the initial complex. The content of the complex in the mixture (in % of the initial one) was calculated from the ratio of the integral intensity of the dibromomethane proton signal (5.09 ppm) to the integral intensity of the doublet at 8.5–3 ppm, chosen for the convenience of integration, since it is observed throughout the recovery and does not overlap with other signals.

RESULTS AND DISCUSSION

Synthesis of the cobalt(III) complex $[\text{Co}(\text{BipyOMe})_2(\text{catechol})\text{ClO}_4]$ (I) was performed in several stages (scheme 1). At the first stage, 4,4' – dimethyl-2,2' – bipyridine was introduced into the complexation reaction with cobalt(II) chloride

hexahydrate [19]. The resulting cobalt(II) complex $[\text{Co}(\text{BipyOMe})_2\text{Cl}_2]$ was oxidized with chlorine gas generated by the reaction of potassium permanganate with concentrated hydrochloric acid [20] to form a cobalt(III) complex $[\text{Co}(\text{BipyOMe})_2\text{Cl}_2]\text{Cl}$ (II). Subsequent interaction of II, with pyrocatechin in the presence of triethylamine and lithium perchlorate resulted in the formation of the target complex I. It was isolated individually and characterized by high-resolution mass spectrometry (fig. 1) ¹H and ¹³C (figs. 2, 3). The appearance in the mass spectrum of the complex of the signal with *m/z* 383.0439 related to the $[\text{Co}(\text{BipyOMe})(\text{catechol})]^+$ ion, is associated with partial fragmentation of the $[\text{Co}(\text{BipyOMe})_2(\text{catechol})]^+$ ion under electrospray ionization conditions. During fragmentation, ions $[\text{Co}(\text{BipyOMe})_2(\text{catechol})]^+$ the formation of $[\text{Co}(\text{BipyOMe})(\text{catechol})]^+$ and $[\text{Co}(\text{BipyOMe})]^+$, which confirms the primary cleavage of the bipyridine ligand under ionization conditions (fig. 1).

The structure of complex I was also confirmed by X-ray diffraction analysis (fig. 4). According to the data obtained in this way, the cobalt(III) ion occupying a particular position in the crystal (the second-order axis passing through the metal ion and the center of the

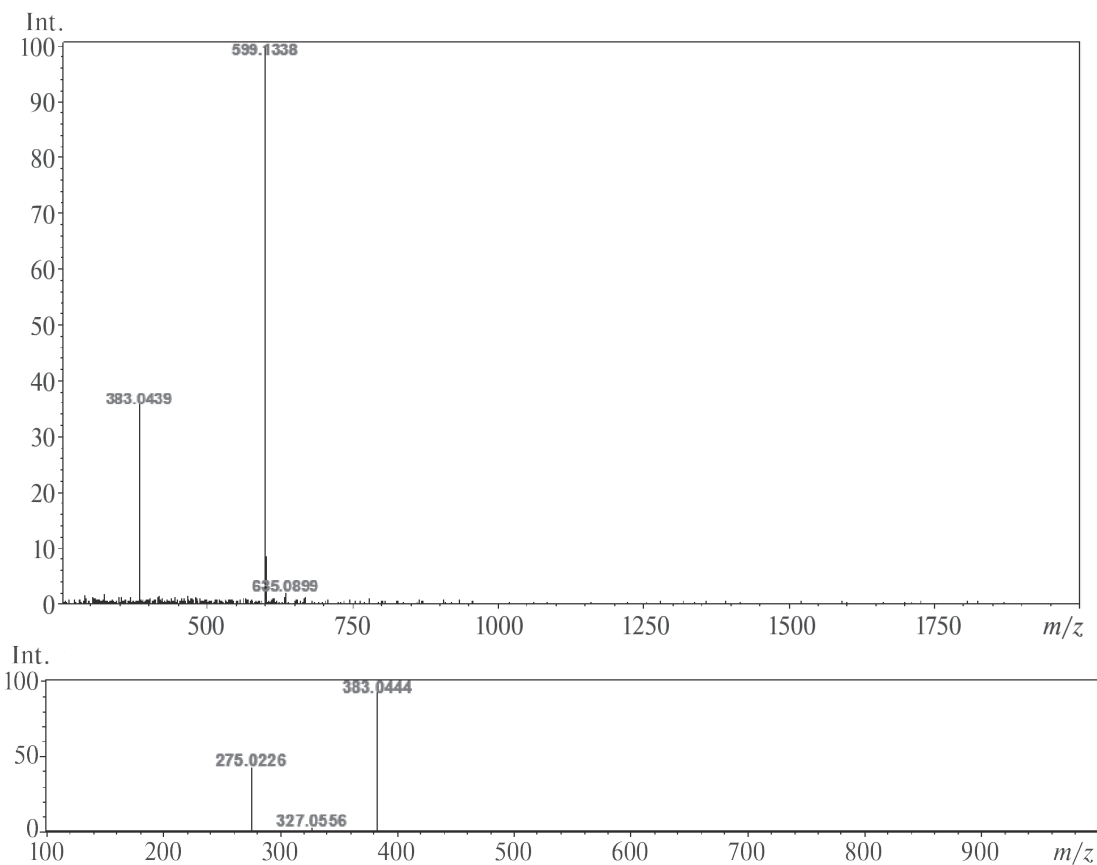


Fig. 1. High-resolution mass spectrum of the $[\text{Co}(\text{BipyOMe})_2(\text{catechol})\text{ClO}_4]$ (I) with electrospray ionization, registered for positive ions (top); MS/MS spectrum obtained for the precursor ion with *m/z* 599.1345 at an impact energy of 18.0–52.0 eV (bottom).

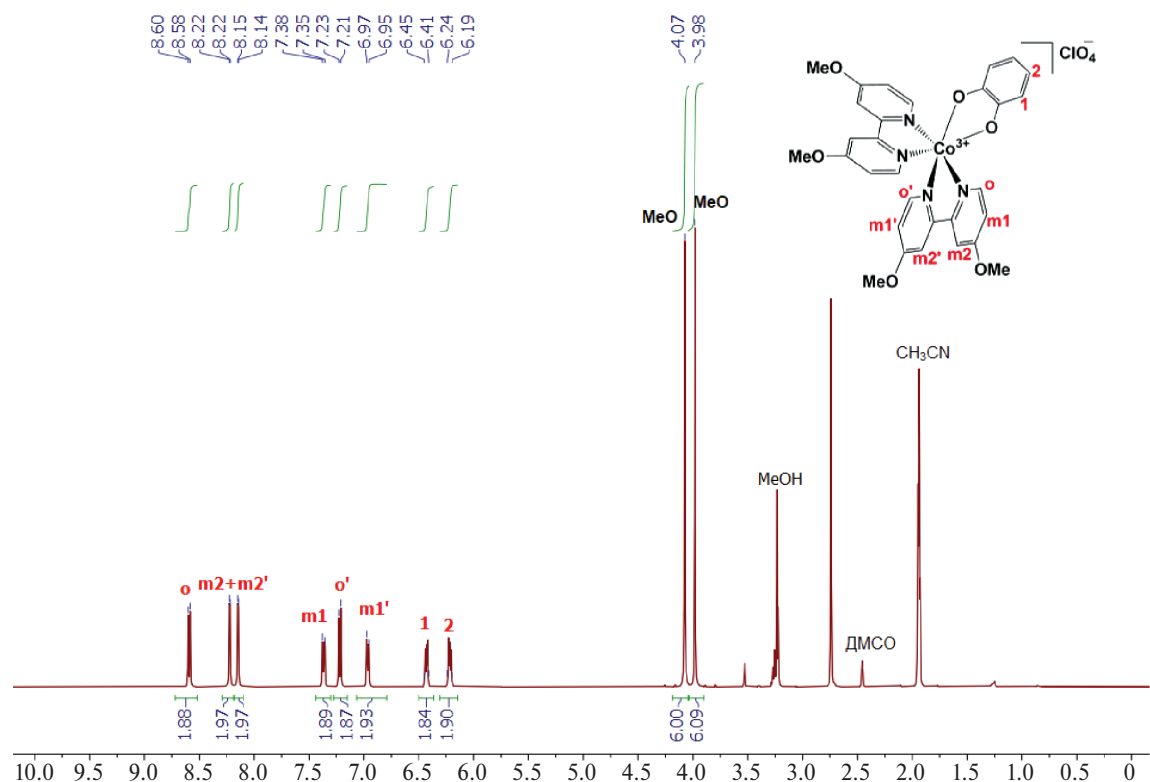


Fig. 2. The ¹H NMR spectrum of complex I in a mixture of CD_3CN - DMSO-d_6 10 : 1 vol. at room temperature.

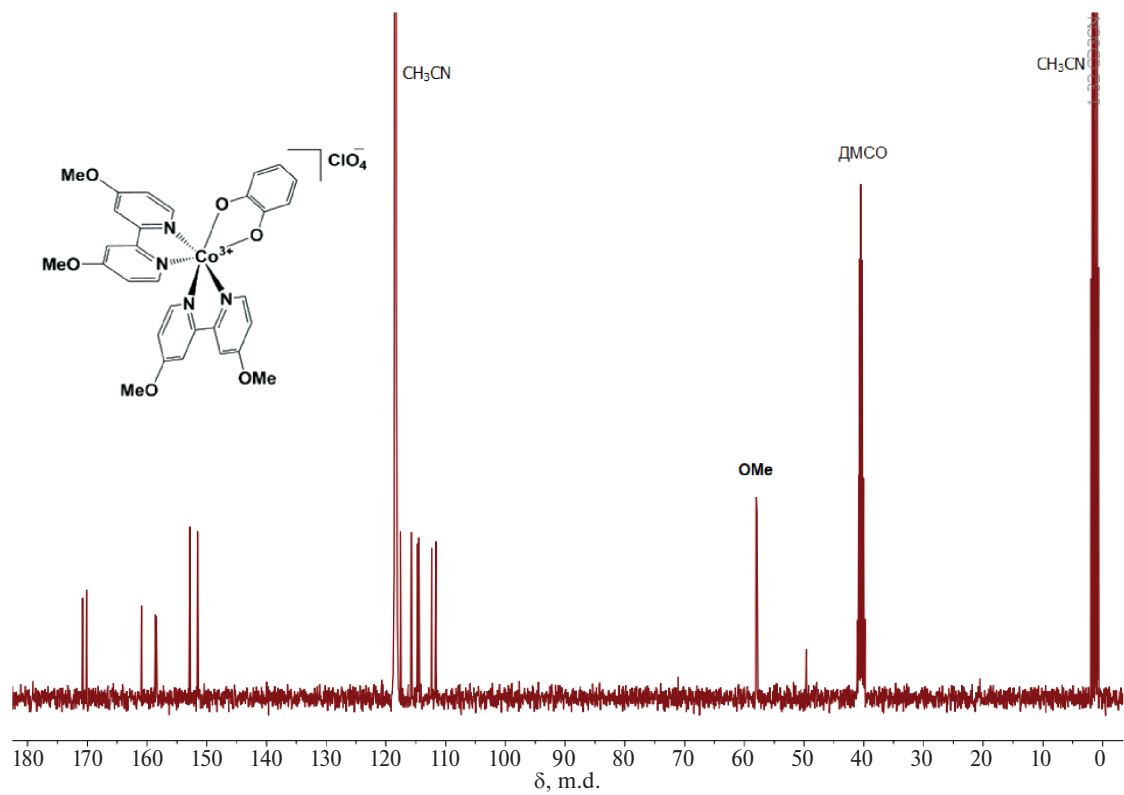


Fig. 3. The ¹³C NMR spectrum of complex I in a mixture of CD_3CN - DMSO-d_6 10 : 1 vol. at room temperature.

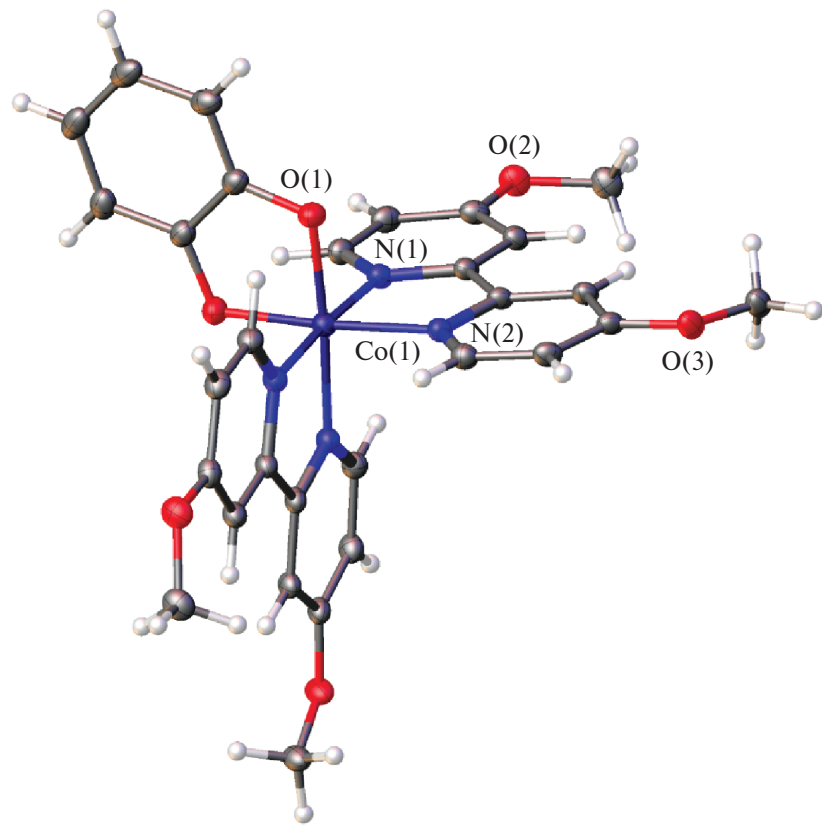


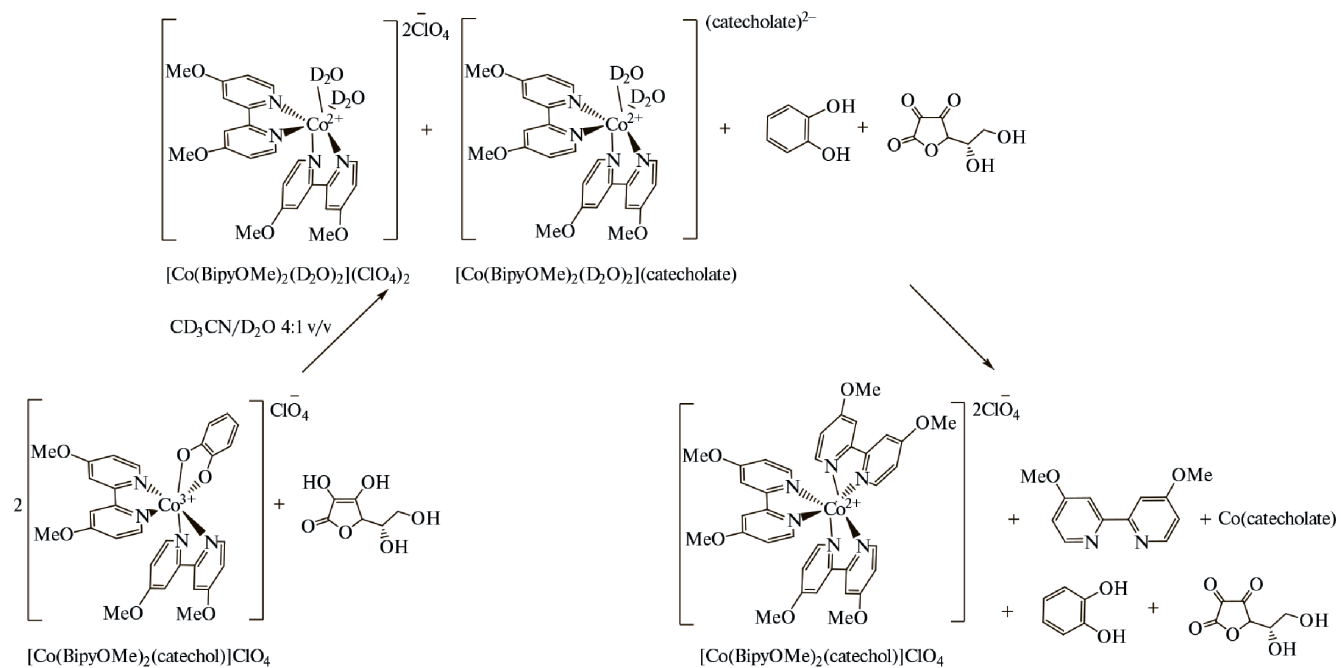
Fig. 4. General view of complex I, illustrating the coordination environment of the cobalt(III) ion. Here and further, perchlorate anions are not shown, and non-hydrogen atoms are represented as ellipsoids of thermal vibrations ($p = 30\%$). The numbering is given only for the metal ion and symmetrically independent heteroatoms.

O...O line of the pyrocatechin dianion) is in low-spin state, which is unambiguously indicated by indicate the Co—N bond lengths $< 1.95 \text{ \AA}$ [23]. Its coordination environment, formed by four nitrogen atoms of two symmetrically equivalent bipyridine ligands (Co-N1.916 (3) and $1.937(3) \text{ \AA}$) and two symmetrically equivalent oxygen atoms of the pyrocatechin dianion (Co-O 1.880(2) \AA), has a shape close to octahedral. This can be confirmed quantitatively by the “symmetry measure” [24], which describes the deviation of the coordination polyhedron COX_6 ($\text{X} = \text{O, N}$) from the ideal octahedron. The lower this value, the better the shape of the polyhedron is described by the corresponding polyhedron. In complex I, the corresponding value estimated on the basis of X-ray diffraction data using the Shape program 2.1 [24], is only 0.296. For comparison, the “symmetry measure” describing the deviation of the coordination polyhedron from an ideal trigonal prism takes a noticeably higher value, equal to 14.887.

To study the reduction of the cobalt(III) I complex *in situ* using NMR spectroscopy, we used the previously developed approach [1–6]. The expected recovery products are shown in figure 2.

Fig. 5 shows ^1H NMR spectra illustrating the dynamics of the reduction of the cobalt(III) I complex

by ascorbic acid. The spectra can be distinguished between diamagnetic (from 0 to 10 ppm) and paramagnetic (from 15 to 100 ppm) regions. The first one contains signals of the initial complex, ascorbic acid, the oxidation product, and free pyrocatechin, and the second one contains signals of the resulting cobalt(II) complexes. As the reaction proceeds, the intensity of signals in the diamagnetic region decreases, and in the paramagnetic region, on the contrary, increases. The expanded diamagnetic region is shown in Fig. 6 in comparison with the ^1H NMR spectrum of pure pyrocatechin. It can be seen that reduction is accompanied by the appearance of two broadened signals in the range of 6.6–6.9 ppm, corresponding to the protons of pyrocatechin released during the reaction. Unlike the signals in the spectrum of pure pyrocatechin, the signals of the reaction mixture do not have a fine structure, which is associated with the formation of paramagnetic cobalt(II) ions as a result of reduction, the presence of which can lead to a broadening of the signals of protons of compounds in the mixture. The number of signals in the paramagnetic region of the NMR spectrum (Fig. 5), their chemical shift, and integral intensity correspond to the complexion $[\text{Co}(\text{BipyOMe})_3]^{2+}$, which is further confirmed by mass



Scheme 2.

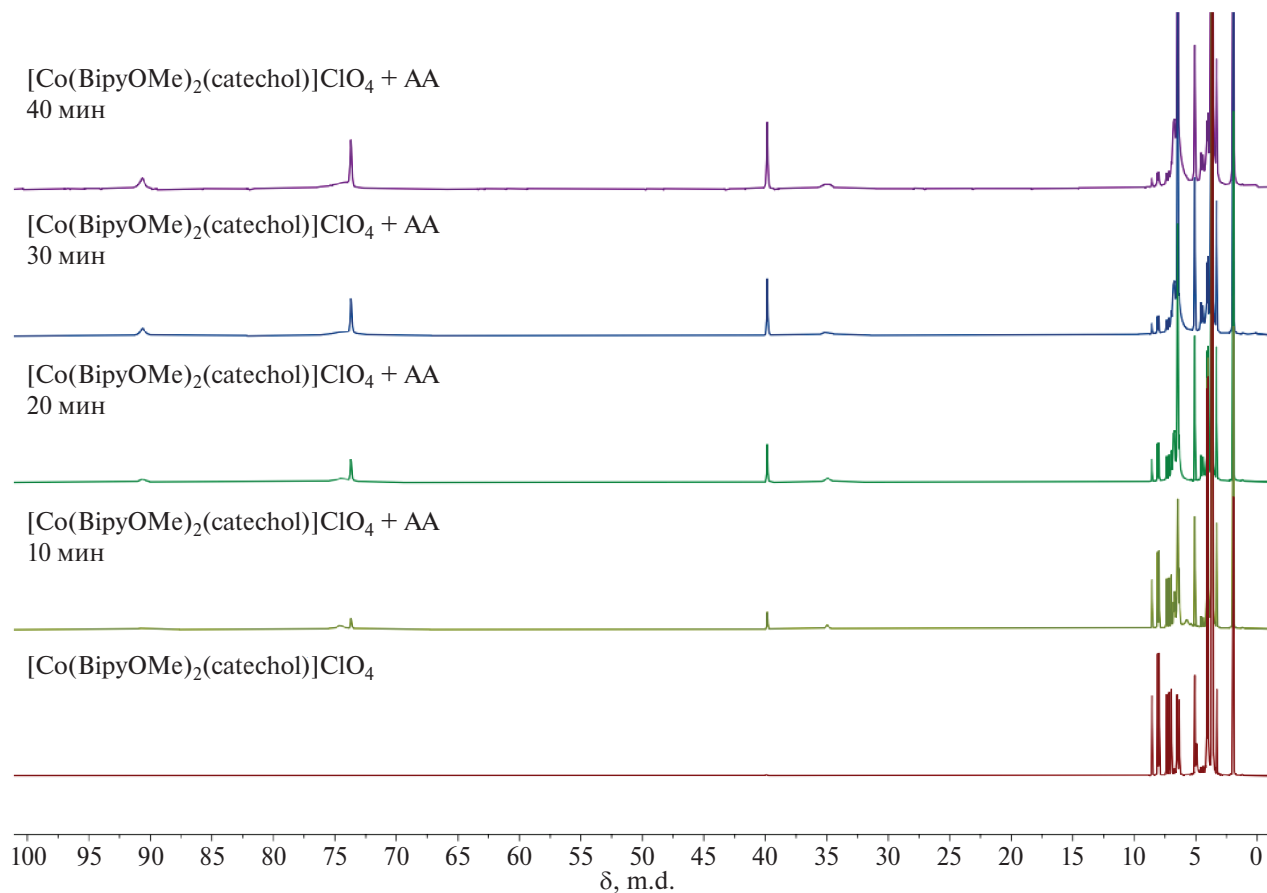


Fig. 5. Dynamics of changes in the ^1H NMR spectrum over time during the reduction of complex I by ascorbic acid in an argon atmosphere (the spectrum was recorded in a mixture of acetonitrile- d_3 and deuterated water, 3.7 : 1 vol.).

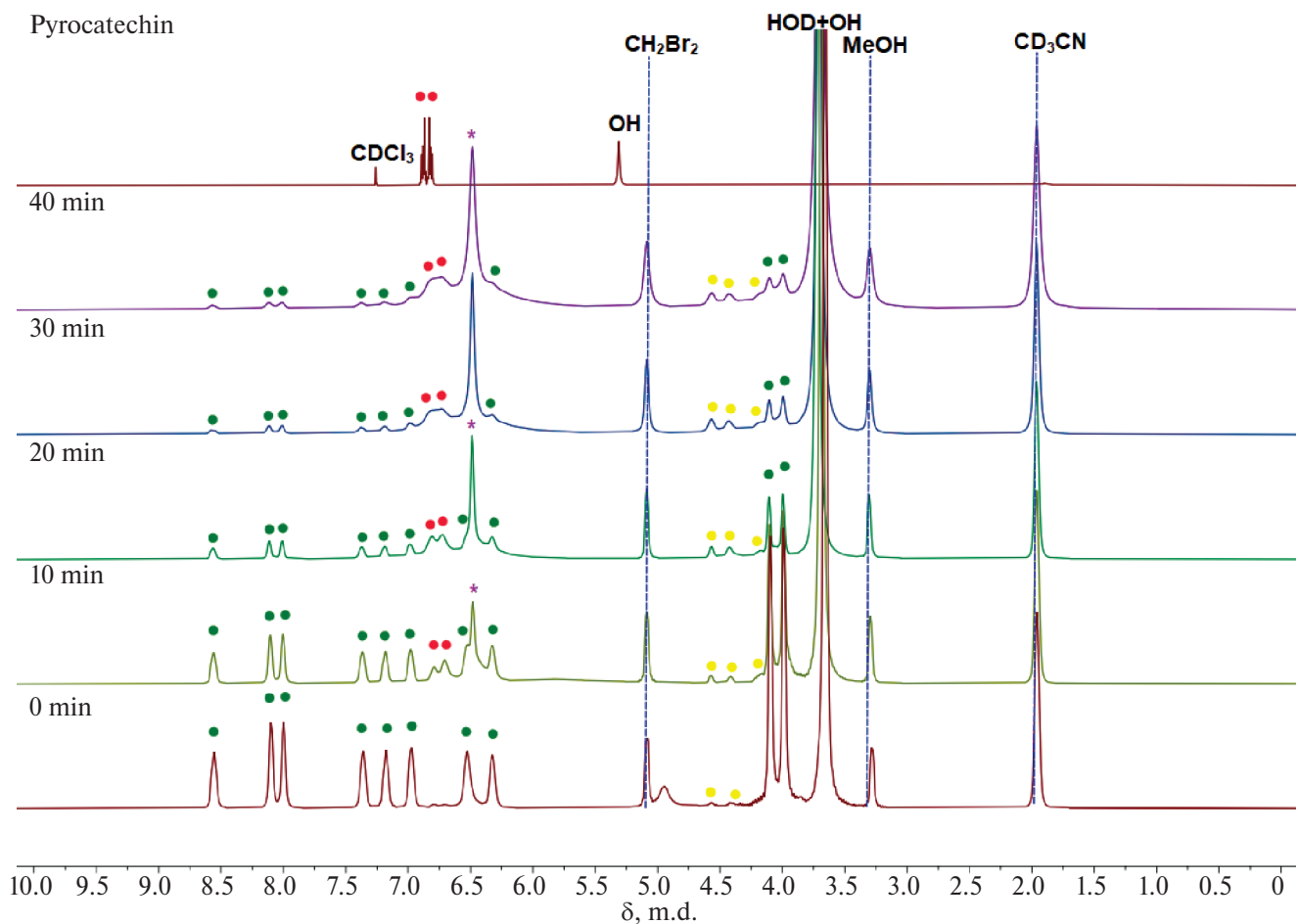


Fig. 6. Dynamics of changes in the diamagnetic region of the ^1H NMR spectrum over time during the reduction of complex I by ascorbic acid in an argon atmosphere (spectrum recorded in a mixture of acetonitrile- d_3d_3 and deuterated water, 3.7: 1 vol.) in comparison with the spectrum of pure pyrocatechin recorded in CDCl_3 (green dots indicate the signals of the initial source material). complex, yellow – ascorbic acid and reduction product, red – pyrocatechin, * – signal of methoxy groups of complex II.

spectrometric analysis of reduction products (fig. 7). To further confirm the formation of the complex ion $[\text{Co}(\text{BipyOMe})_3]^{2+}$ in situ in an NMR ampoule, complex III was obtained by adding a stoichiometric amount of the ligand to a solution of cobalt perchlorate in deuterated acetonitrile. In the spectrum of the resulting complex, four signals are observed with chemical shifts close to the values of the shifts of the corresponding signals in the spectrum of the reaction mixture (fig. 8). The difference in chemical shifts may be due to the presence of additional counterions in the reaction mixture other than the perchlorate anion (for example, the catecholate anion, scheme 2), and as well as other cobalt(II) complexes, whose low-intensity signals are also observed in the paramagnetic region of the spectrum. Thus, the reduction of the cobalt(III) I complex proceeds with the formation of the cobalt(II) $[\text{Co}(\text{BipyOMe})_3]\text{A}$ complex (A = perchlorate-anion, catecholate-dianion) and is accompanied by the

release of a pyrocatechin molecule. A similar reduction mechanism was observed for cobalt(III) complexes with 6,7-dihydroxycoumarin containing bipyridine or phenanthroline instead of the 4,4' – dimethyl-2,2' – bipyridine ligand [16].

Fig. 9 shows the dependence of the degree of conversion of complex I during reduction by ascorbic acid in an argon atmosphere, obtained by analyzing *in situ* NMR spectroscopy data. You can see that the conversion rate gradually increases over time, reaching 90% by 30 minutes, after which it stops changing. The dependence of the natural logarithm of the initial complex concentration on time is approximated by a straight line with a confidence coefficient close to unity (Fig. 9). Linear approximation indicates the first order of the limiting stage of the complex recovery process. Most likely, this step is the release of a pyrocatechin molecule. In the Fig. 9, the rate constant of the reduction process of complex I by ascorbic acid in an

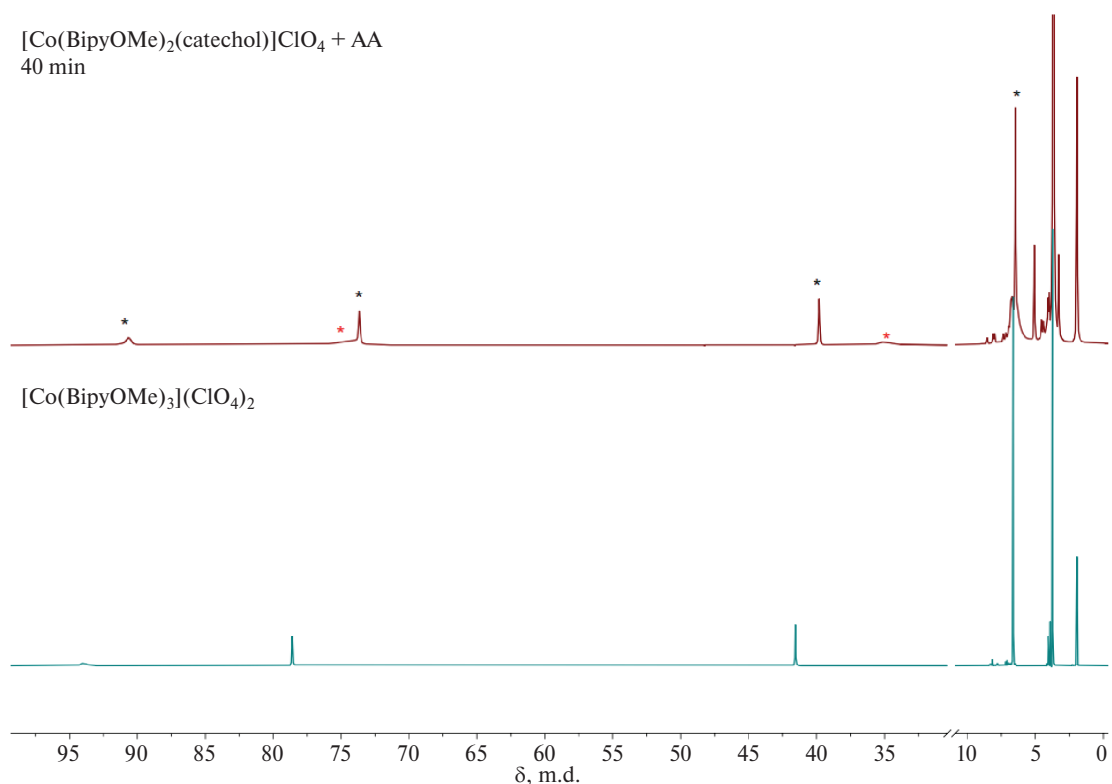


Fig. 7. Comparison of the ¹H NMR spectra of complex II and the reaction mixture 40 min after the addition of ascorbic acid to I (black * denotes signals of $\text{Co}(\text{BipyOMe})\text{protons}_3^{2+}$, red * — signals of protons of the impurity cobalt (II) complex).

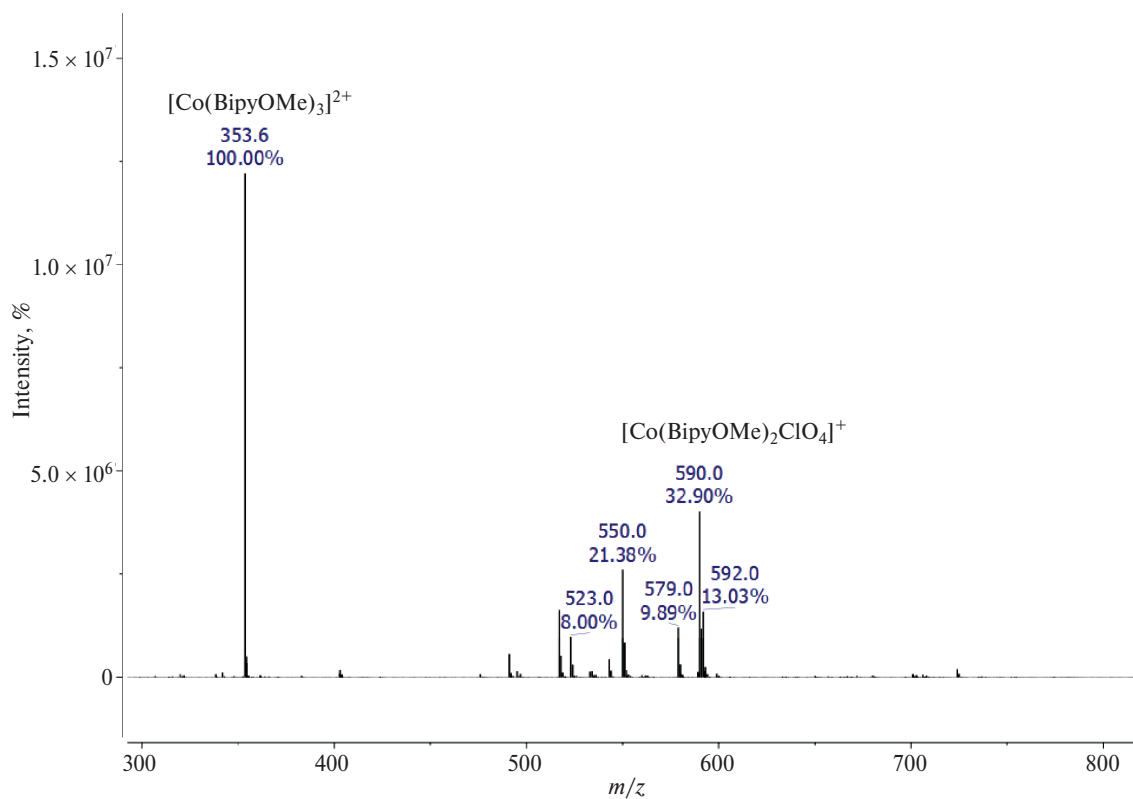


Fig. 8. Mass spectrum of complex I reduction products with ascorbic acid recorded for positive ions.

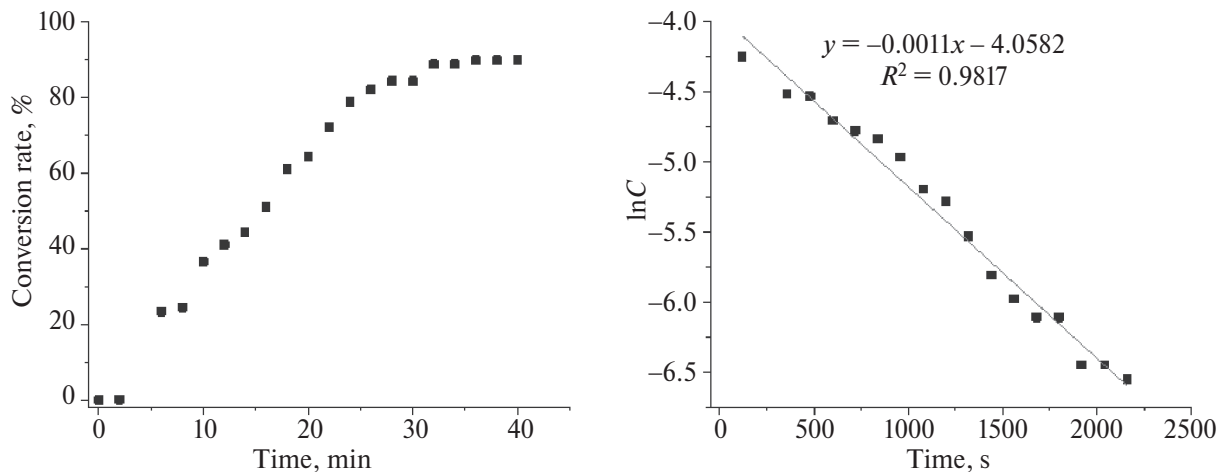


Fig. 9. Dependence of the conversion rate (left) and the logarithm of the concentration (right) of complex I on the reaction time during reduction with ascorbic acid in an argon atmosphere.

inert atmosphere at 40°C was estimated to be $1.1 \times 10^{-3} \text{ s}^{-1}$. The obtained rate constant value is lower in comparison with the reduction constant of the complex $[\text{Co}(\text{Bipy})_2(\text{catechol})]\text{ClO}_4$, which is $2.0 \times 10^{-3} \text{ sec}^{-1}$ [17]. A similar decrease in the rate constant is observed for complexes with 6,7-dihydroxycoumarin, which makes it possible to extend this trend of decreasing the rate constant when introducing methoxy substituents into the bipyridine core and to complexes with other лекарственными мидргус.

Thus, we synthesized a new redox-active cobalt (III) complex $[\text{Co}(\text{BipyOMe})_2(\text{catechol})]\text{ClO}_4$ (I), which contains the pyrocatechin dianion as one of the ligands. The reduction of the synthesized complex by ascorbic acid in an inert atmosphere *in situ* by NMR spectroscopy is studied. It is shown that reduction results in the formation of a cobalt(II) complex with the composition $[\text{Co}(\text{BipyOMe})_3]^{2+}\text{A}^{2-}$. The limiting stage of the recovery process of the studied complex is of the first order, and the rate constant of this process is only $1.1 \times 10^{-3} \text{ s}^{-1}$, which is a rather low value in comparison with the optimal rate constants for the release of drugs from various carriers in the body [25]. The low value of the rate constant indicates the need for further optimization of the molecular structure of the studied complex to give it properties that ensure rapid redox-activated drug delivery to tumor cells.

CONFLICT OF INTERESTS

The authors state that they have no conflict of interest.

ACKNOWLEDGEMENTS

X-ray diffraction analysis, NMR spectroscopy, and mass spectrometry data were obtained using the

scientific equipment of the Center for Molecular Structure Research, INEOS RAS, with the support of the Ministry of Science and Higher Education of the Russian Federation (State Task No. 075-00277-24-00).

FUNDING

This work was supported by the Russian Science Foundation (grant No. 22-73-10193).

REFERENCES

1. Vaupel P., Schlenger K., Knoop C. et al. // Cancer Research. 1991. V. 51. P. 3316.
2. Brown J.M., Wilson W.R. // Nature Reviews Cancer. 2004. V. 4. P. 437.
3. Denny W.A. // Cancer Invest. 2004. V. 22. P. 604.
4. Kratz F., Müller I.A., Ryppa C. et al. // ChemMedChem. 2008. V. 3. P. 20.
5. Renfrew A.K. // Metallomics. 2014. V. 6. P. 1324.
6. Hall M.D., Failes T.W., Yamamoto N. et al. // Dalton Trans. 2007. P. 3983.
7. Palmeira-Mello M.V., Caballero A.B., Ribeiro J.M. et al. // J. Inorg. Biochem. 2020. V. 211. P. 111211.
8. Tsitovich P.B., Spernyak J.A., Morrow J.R. // Angew. Chem. Int. Ed. 2013. V.52. P. 13997.
9. Teicher B.A., Abrams M.J., Rosbe K.W. et al. // Cancer Res. 1990. V. 50. P. 6971.
10. Ware D.C., Denny W.A., Clark G.R. // Acta Crystallogr. C. 1997. V. 53. P. 1058.
11. Failes T.W., Hambley T.W. // Dalton Trans. 2006. V. 1895.
12. Ahn G-One, Botting K.J., Patterson A.V. et al. // Biochem. Pharmacol. 2006. V. 71. P. 1683.

13. *Chang J.Y-C., Stevenson R.J., Lu G.-L. et al.* // Dalton Trans. 2010. V. 39. P. 11535.
14. *Karnthaler-Benbakka C., Groza D., Kryeziu K. et al.* // Angew. Chem. Int. Ed. 2014. V. 53. P. 12930.
15. *McPherson J.N., Hogue R.W., Akogun F.S. et al.* // Inorg. Chem. 2019. V. 58. P. 2218.
16. *Khakina E.A., Nikovsky I.A., Babakina D.A. et al.* chemistry. 2023. V. 49. C. 27
17. *Nikovskiy I.A., Spiridonov K.A., Dan'shina A.A. et al.* // Russ. J. Coord. Chem. 2024. V. 50. P. 195. <https://doi.org/10.1134/S1070328423600699>
18. *Spiridonov K.A., Nikovskii I.A., Antoshkina E.P. et al.* // Russ. J. Coord. Chem. 2024. V. 50. P. 163. <https://doi.org/10.1134/S1070328423600663>
19. *Vlcek A.A.* // Inorg. Chem. 1967. V. 6. P. 1425.
20. *Ma D.-L., Wu C., Cheng S.-S. et al.* // Int. J. Mol. Sci. 2019. V. 20. P. 341.
21. *Sheldrick G.M.* // Acta Crystallogr. A. 2008. V. 64. P. 112.
22. *Dolomanov O.V., Bourhis L.J., Gildea R.J. et al.* // J. Appl. Cryst. 2009. V. 42. P. 339.
23. *Stamatatos T.C., Bell A., Cooper P. et.al.* // Inorg. Chem. Commun. 2005 V. 8 P. 533.
24. *Alvarez S.* // Chem. Rev. 2015 V. 115 P. 13447.
25. *Reddy O.S., Subha M.C.S., Jithendra T. et al.* // Int. J. App. Pharm. 2019. V. 11. P. 71.

